

Stability of solitary waves and vortices in a 2D nonlinear Dirac model

Jesús Cuevas–Maraver

*Grupo de Física No Lineal, Departamento de Física Aplicada I,
Universidad de Sevilla. Escuela Politécnica Superior, C/ Virgen de África, 7, 41011-Sevilla, Spain
Instituto de Matemáticas de la Universidad de Sevilla (IMUS). Edificio Celestino Mutis. Avda. Reina Mercedes s/n, 41012-Sevilla, Spain*

P. G. Kevrekidis

*Department of Mathematics and Statistics, University of Massachusetts, Amherst, MA 01003-4515, USA and
Center for Nonlinear Studies and Theoretical Division,
Los Alamos National Laboratory, Los Alamos, New Mexico 87545, USA*

Avadh Saxena

*Center for Nonlinear Studies and Theoretical Division,
Los Alamos National Laboratory, Los Alamos, New Mexico 87545, USA*

Andrew Comech

*Department of Mathematics, Texas A&M University, College Station, TX 77843-3368 and
Institute for Information Transmission Problems, Moscow 127994, Russia*

Ruomeng Lan

Department of Mathematics, Texas A&M University, College Station, TX 77843-3368

(Dated: May 10, 2022)

We explore a prototypical *two-dimensional* model of the nonlinear Dirac type and examine its solitary wave and vortex solutions. In addition to identifying the stationary states, we provide a systematic spectral stability analysis, illustrating the potential of spinor solutions consisting of a soliton in one component and a vortex in the other to be neutrally stable in a wide parametric interval of frequencies. Solutions of higher vorticity are generically unstable and split into lower charge vortices in a way that preserves the total vorticity. These results pave the way for a systematic stability and dynamics analysis of higher dimensional waveforms in a broad class of nonlinear Dirac models and a comparison revealing nontrivial differences with respect to their better understood non-relativistic analogue, the nonlinear Schrödinger equation.

Introduction. In the context of dispersive nonlinear wave equations, admittedly the prototypical model that has attracted a wide range of attention in optics, atomic physics, fluid mechanics, condensed matter and mathematical physics is the nonlinear Schrödinger equation (NLS) [1–7]. By comparison, far less attention has been paid to its relativistic analogue, the nonlinear Dirac equation (NLD) [8], despite its presence for almost 80 years in the context of high-energy physics [9–13]. This trend is slowly starting to change, arguably, for three principal reasons. Firstly, significant steps have been taken in the nonlinear analysis of stability of such models [14–19], especially in the one-dimensional (1d) setting. Secondly, computational advances have enabled a better understanding of the associated solutions and their dynamics [20–24]. Thirdly, and perhaps most importantly, NLD starts emerging in physical systems which arise in a diverse set of contexts of considerable interest. These contexts include, in particular, bosonic evolution in honeycomb lattices [25, 26] and a growing class of atomically thin 2d Dirac materials [27] such as graphene, silicene, germanene and transition metal dichalcogenides [28]. Recently, the physical aspects of nonlinear optics, such as the light propagation in honeycomb photorefractive lattices (the so-called photonic graphene) [29, 30] have prompted the consideration of intriguing dynamical features such as conical diffraction in 2d honeycomb lattices [31].

These physical aspects have also led to a discussion of potential 2d solutions of NLD in [25, 26]. However, a systematic and definitive characterization of the spectral stability and nonlinear dynamical evolution of the prototypical coherent structures in NLD models is still lacking, to the best of our knowledge. Hence, the present work is dedicated to offering analytical and numerical insights into these crucial physical aspects of higher-dimensional nonlinear Dirac equations with regard to the physical relevance and potential observability of such waveforms. As our model of choice, in order to also compare and contrast with the multitude of existing 1d results, we will select the well-established Soler model [32] (known in 1d as the Gross–Neveu model [33]), which is a Dirac equation with scalar self-interaction. Such self-interaction is based on including into the Lagrangian density the power of the quantity $\bar{\psi}\psi$ (which transforms as a scalar under the Lorentz transformations):

$$\mathcal{L}_{\text{Soler}} = \bar{\psi} (i\gamma^\mu \partial_\mu - m) \psi + \frac{g}{2} (\bar{\psi}\psi)^2, \quad (1)$$

where $m > 0$, $g \in \mathbb{R}$, $\psi(x, t) \in \mathbb{C}^N$, $x \in \mathbb{R}^n$, and γ^μ , $0 \leq \mu \leq n$ are Dirac γ -matrices. Above, we use the standard notation $\bar{\psi} = \psi^* \gamma^0$. The model is generalized in the spirit of [22], by using $(\bar{\psi}\psi)^{k+1}$ with $k \in \mathbb{N}$ or even $k > 0$; we only consider the standard cubic case $k = 1$ and the focusing

nonlinearity $g > 0$; without loss of generality, it is enough to consider $g = 1$. An alternative model is the massive Thirring model with vector self-interaction [12], where the nonlinear term in the Lagrangian is based on the scalar quantity $J_\mu J^\mu$ built from the Lorentz vector $J^\mu = \bar{\psi} \gamma^\mu \psi$ which represents the charge-current density. It is important to point out here that in two spatial dimensions these two models coincide. Indeed, using the Dirac matrices $\gamma^0 = \sigma_3$, $\gamma^j = \sigma_3 \sigma_j$, $j = 1, 2$, and using the identity

$$(\psi^* \psi)^2 = (\psi^* \sigma_1 \psi)^2 + (\psi^* \sigma_2 \psi)^2 + (\psi^* \sigma_3 \psi)^2, \quad \psi \in \mathbb{C}^2,$$

we compute that in 2d these two scalar quantities coincide:

$$J_\mu J^\mu = (\psi^* \psi)^2 - (\psi^* \sigma_1 \psi)^2 - (\psi^* \sigma_2 \psi)^2 = (\bar{\psi} \psi)^2.$$

Our results show that the NLD in 2d admits different solutions involving a structure of vorticity $S \in \mathbb{Z}$ in the first spinor component, with the other spinor component bearing a vorticity $S + 1$. We identify such solutions for $S = 0, 1, \dots$. Our numerical computation of the spectrum of the corresponding linearization operator reveals that *only* the $S = 0$ solutions can be spectrally stable, and that this stability takes place in a rather wide interval of the frequency of the solitary waves. On the contrary, we find that the states of higher vorticity are generically unstable. Complementing the stability analysis results, our direct dynamical evolution studies show that the unstable higher vorticity solutions break up into lower vorticity waveforms, yet conserving the total vorticity.

Theoretical Setup. We start from the prototypical 2d nonlinear Dirac equation system in rectangular coordinates, derived from the Lagrangian density (1) with $k = 1$ and $m = g = 1$:

$$\begin{aligned} i\partial_t \psi_1 &= -(i\partial_x + \partial_y) \psi_2 + f(\psi_1, \psi_2) \psi_1, \\ i\partial_t \psi_2 &= -(i\partial_x - \partial_y) \psi_1 - f(\psi_1, \psi_2) \psi_2, \end{aligned} \quad (2)$$

where ψ_1, ψ_2 are the components of the spinor $\psi \in \mathbb{C}^2$ and the nonlinearity is given by $f(\psi_1, \psi_2) = 1 - (|\psi_1|^2 - |\psi_2|^2)$. We simplify our analysis by seeking solutions in the setting of polar coordinates, where Eq. (2) takes the form

$$\begin{aligned} i\partial_t \psi_1 &= -e^{-i\theta} \left(i\partial_r + \frac{\partial_\theta}{r} \right) \psi_2 + f(\psi_1, \psi_2) \psi_1, \\ i\partial_t \psi_2 &= -e^{i\theta} \left(i\partial_r - \frac{\partial_\theta}{r} \right) \psi_1 - f(\psi_1, \psi_2) \psi_2. \end{aligned} \quad (3)$$

We are interested in stationary solutions of the form $\psi(\vec{r}, t) = \exp(-i\Lambda t) \phi(\vec{r})$ with

$$\phi(\vec{r}) = \begin{pmatrix} v(r) e^{iS\theta} \\ i u(r) e^{i(S+1)\theta} \end{pmatrix}, \quad (4)$$

where $S \in \mathbb{Z}$ can be cast as the vorticity of the first spinor component, while the vorticity associated with the second spinor component is $S + 1$. Once stationary solutions have been identified, to explore the stability of such solutions, we introduce a perturbation in a fashion similar to [34]:

$$\psi(\vec{r}, t) = e^{-i\Lambda t} [\phi(\vec{r}) + \delta\xi(\vec{r}, t)], \quad (5)$$

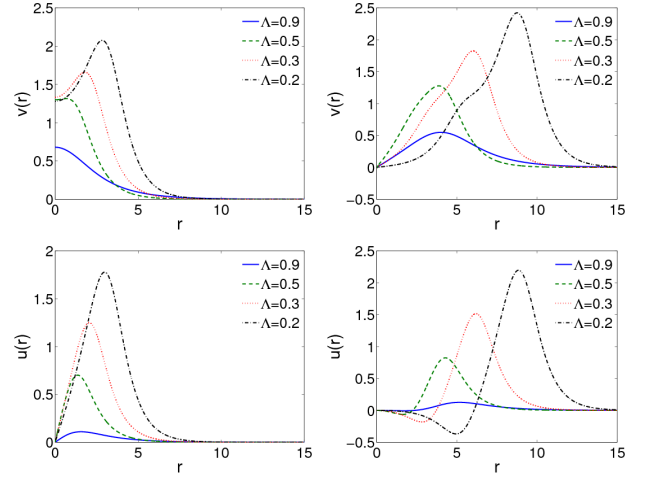


FIG. 1: Radial profiles of the spinor components for (left) $S = 0$ solitons and (right) $S = 1$ vortices for different values of Λ .

with $\xi(\vec{r}, t)$ being

$$\xi(\vec{r}, t) = \begin{pmatrix} [a_1(r) e^{iq\theta} e^{i\omega t} + b_1(r) e^{-iq\theta} e^{-i\omega^* t}] e^{iS\theta} \\ i [a_2(r) e^{iq\theta} e^{i\omega t} + b_2(r) e^{-iq\theta} e^{-i\omega^* t}] e^{i(S+1)\theta} \end{pmatrix}$$

and $q \in \mathbb{Z}$. Thus, stability can be determined by solving to $O(\delta)$ the eigenvalue problem of the form $\omega_q(a_1, a_2, b_1^*, b_2^*)^T = L_q(a_1, a_2, b_1^*, b_2^*)^T$; further details of the stationary equations and the full form of the stability problem are presented in [35]. Notice that the angular decomposition of the spectrum necessitates the solution of the relevant spectral problem for each q and then the superposition of these partial spectra to construct the full spectrum. Lastly, when the solutions are found to be spectrally unstable, we resort to dynamical simulations of Eqs. (2) in order to explore the outcome of the unstable evolution.

Numerical results. We have analyzed the existence and stability of solitary waves ($S = 0$, with its first component radially symmetric and the second component having vorticity 1) and vortex solutions ($S = 1$, with its components having vorticities of order one and two, respectively). Both solitary waves and vortex solutions exist in the frequency interval $\Lambda \in (0, 1)$; we recall that without loss of generality we fixed $m = 1$. An intriguing feature of the relevant waveforms is that both the radial profile of the solitary waves and that of the vortices possess a maximum that shifts from $r = 0$ to a larger r when Λ approaches zero (see Fig. 1), in a way reminiscent of the corresponding 1d solitary wave structures [22]. Here the relevant state will feature a stationary bright intensity ring. In order to obtain such coherent structures, we have made use of fixed point algorithms for solving Eq. (3) as discussed also in the Supplementary Material, implementing a Chebyshev collocation method for the partial derivatives. We have modified the method proposed in [36] to take into account the angular structure of the spinor components.

The most interesting results concern the stability of soli-

tons and vortices. Figure 2 shows the dependence of the real and imaginary parts of the eigenfrequencies with respect to the stationary solution frequency Λ . The bottom panels of the figure show examples of the spectral plane of unstable solutions. From the spectral dependencies we can deduce several features of the 2d NLD equation: (1) The 2d NLS equation is charge-critical, and the zero eigenfrequency is degenerate: it has higher algebraic multiplicity. In the NLD case, however, this degeneracy is resolved: in the $S = 0$ case, two eigenfrequencies with $q = 0$ start at the origin when $\Lambda = 1$ and move out of the origin for $\Lambda \lesssim 1$. (2) The $U(1)$ symmetry and the translation symmetry of the model result in zero eigenfrequencies with $q = 0$ and $|q| = 1$, respectively (in both $S = 0$ and $S = 1$ cases). (3) as in the 1d NLD equation, there is also the eigenfrequency $\omega = 2\Lambda$ which is associated with the $SU(1, 1)$ symmetry of the model [37]. This eigenfrequency corresponds to $q = -(2S + 1)$, i.e., to a highly excited linearization eigenstate. (4) Contrary to the 1d case, where the solitary waves corresponding to any $\Lambda < 1$ are stable, the $S = 0$ soliton is unstable for $\Lambda < 0.121$ because of the emergence of nonzero imaginary part eigenfrequencies via a Hamiltonian Hopf bifurcation in the $|q| = 2$ spectrum at $\Lambda = 0.121$. Another Hopf bifurcation occurs corresponding to $|q| = 3$ (at $\Lambda = 0.0885$), then yet another one corresponding to $|q| = 4$. For the sake of clarity, we only plot the real part of the spectra for $|q| \leq 2$ and their imaginary part for $|q| \leq 4$. Another relevant observation concerns the fact that the $S = 0$ solution is unstable only for sufficiently low Λ in NLD, while it does *not* share the instability of solitary waves in its (mass critical) NLS limit as $\Lambda \rightarrow 1$. This is presumably related to the lifting of the corresponding degeneracy, although this is a feature worthy of further investigation. (5) $S = 1$ vortices are unstable for every Λ , because of the presence in the spectrum of quadruplets of complex eigenfrequencies. These quadruplets appear and disappear for all values of q , via direct and inverse Hopf bifurcations. (6) The spectrum for $S = 2$ vortex is quite similar to that of $S = 1$; for this reason, we do not analyze it further.

In order to analyze the result of instabilities (for $\Lambda \leq 0.121$ in the case of $S = 0$ and for different Λ 's for $S = 1$), we have probed the dynamics of unstable solutions directly. To this effect, we have used a Fourier collocation scheme, in order to perform the relevant computations efficiently. This, in turn, involves a conversion of the solution to rectangular coordinates. Prototypical examples of unstable $S = 0$ solitons and $S = 1$ vortices are shown in Figs. 3 and 4. As it can be observed, the $S = 0$ solitary waves spontaneously amplify perturbations breaking the radial symmetry in their density and, as a result, become elliptical and rotate around the center of the circular density of the original soliton in line with the expected amplification of the $q = 2$ unstable eigenmode. On the other hand, the $S = 1$ vortices split into three smaller ones. Let us mention that in the latter case, the first spinor component splits into solitons without vorticity whereas the second component splits into three solitary waves. This preserves the total vorticity across the two components, as is also shown in

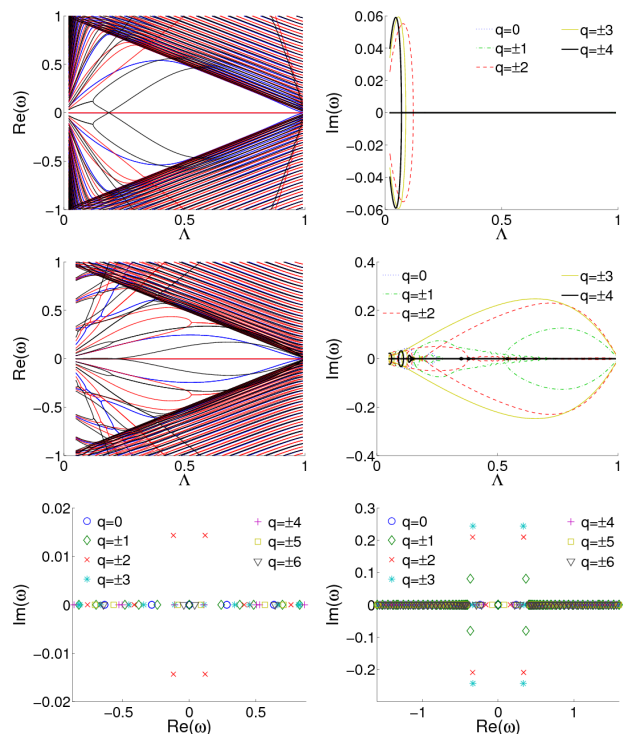


FIG. 2: Dependence of the (left) real and (right) imaginary part of the eigenfrequencies with respect to Λ . Top (respectively, middle) panels correspond to $S = 0$ solitons ($S = 1$ vortices). For the sake of clarity, we only included the values $|q| \leq 2$ for the real part and $|q| \leq 4$ for the imaginary part. In the former case, the real part of the eigenfrequencies for $q = 0$, $q = \pm 1$ and $q = \pm 2$ are represented by, respectively, blue, red and black lines. The bottom panels show the spectral planes of the $S = 0$ soliton with $\Lambda = 0.12$ (left) and the $S = 1$ vortex with $\Lambda = 0.60$ (right).

the top panel of Fig. 4. Along a similar vein, the instability of an $S = 2$ state in the first component (coupled with $S + 1 = 3$ in the second one) eventually leads to the emergence of five $(0, 1)$ pairs, again preserving the total vorticity.

Conclusions and Future Challenges. In this work, we have provided a unique glimpse into the potential of nonlinear Dirac equations to support solitary waves and vortices in higher dimensional settings. We have illustrated that prototypical solitary waves of vorticity $S = 0$ in one spinor component and $S = 1$ in the other are, in fact, spectrally *stable within a large parametric interval*, suggesting their experimental plausibility for observation in physical settings emerging in atomic [25, 26] and optical physics [29, 30] as well as in condensed matter physics, e.g. in Dirac materials [27]. We also highlighted the significant difference thereof from the non-relativistic limit of the focusing NLS equation, where such solutions are *generically* unstable. When the relevant solutions were found to be unstable, their detailed dynamical evolution suggested their breathing (quasi-periodic) oscillation for the $S = 0$ case, and their splitting into lower charge configurations for the case of $S = 1$ and $S = 2$.

It is both of interest and relevance to extend the present con-

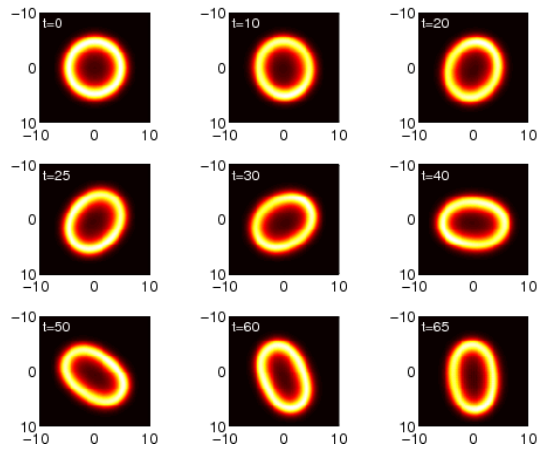


FIG. 3: Snapshots showing the evolution of the density of an unstable $S = 0$ soliton with $\Lambda = 0.12$. In order to accelerate the simulation, a perturbation in the direction of the unstable eigenmode with $q = 2$ has been added to the stationary soliton as initial condition. The soliton which initially had a circular shape becomes elliptical and rotates around the center of the original soliton.

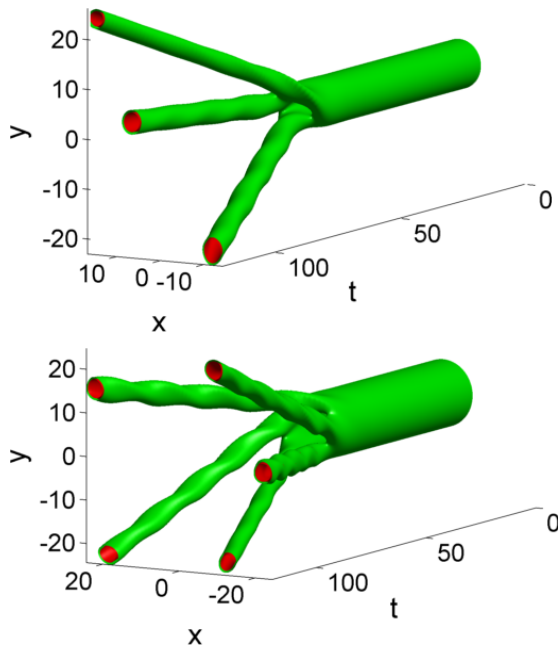


FIG. 4: Isosurfaces for the density of an $S = 1$ (top) and $S = 2$ (bottom) vortex with $\Lambda = 0.6$. In order to accelerate the simulation, a random perturbation has been added. The initial vortex splits into $2S + 1$ splinters which move in different directions.

considerations to a wide range of additional physically relevant settings. From a mathematical physics perspective, it will be of interest to examine whether spectral properties of such solutions can be captured analytically and their potentially unstable eigendirections identified. It would also be useful to extend present considerations to the 3d setting and examine whether at least solitary wave structures of $S = 0$ can be stable there. This is especially timely given that the 3d analogue of photonic graphene has been experimentally realized very

recently [38]. The wide parametric stability interval of the 2d NLD solitary wave solutions renders the latter model far more promising, in that regard, in comparison to the corresponding NLS case. On the other hand, it would also be of interest to explore models associated with different nonlinearities, including the case of honeycomb lattices in atomic and optical media discussed previously, or, e.g., those stemming from wave resonances in low-contrast photonic crystals [39].

Acknowledgments. The research of A. Comech was carried out at the Institute for Information Transmission Problems of the Russian Academy of Sciences at the expense of the Russian Foundation for Sciences (project 14-50-00150). AS was supported in part by the U. S. Department of Energy. P.G.K. gratefully acknowledges the support of the US-NSF under the award DMS-1312856, and of the ERC under FP7, Marie Curie Actions, People, International Research Staff Exchange Scheme (IRSES-605096).

-
- [1] Yu.S. Kivshar and G.P. Agrawal, *Optical solitons: from fibers to photonic crystals*, Academic Press (San Diego, 2003).
 - [2] L.P. Pitaevskii and S. Stringari, *Bose-Einstein Condensation*, Oxford University Press (Oxford, 2003).
 - [3] C.J. Pethick and H. Smith, *Bose-Einstein condensation in dilute gases*, Cambridge University Press (Cambridge, 2002).
 - [4] P.G. Kevrekidis, D.J. Frantzeskakis, and R. Carretero-González, *The defocusing nonlinear Schrödinger equation: from dark solitons and vortices to vortex rings*. SIAM, Philadelphia (2015).
 - [5] M.J. Ablowitz, B. Prinari and A.D. Trubatch, *Discrete and Continuous Nonlinear Schrödinger Systems*, Cambridge University Press (Cambridge, 2004).
 - [6] C. Sulem and P.L. Sulem, *The Nonlinear Schrödinger Equation*, Springer-Verlag (New York, 1999).
 - [7] J. Bourgain, *Global Solutions of Nonlinear Schrödinger Equations*, American Mathematical Society (Providence, 1999).
 - [8] F.M. Toyama, Y. Hosono, B. Ilyas, and Y. Nogami, J. Phys. A: Math. Gen. **27**, 3139 (1994).
 - [9] D. D. Ivanenko, Zh. Éksp. Teor. Fiz **8**, 260 (1938).
 - [10] R. Finkelstein, R. LeLevier, and M. Ruderman, Phys. Rev. **83**, 326 (1951).
 - [11] W. Heisenberg, Rev. Mod. Phys. **29**, 269 (1957).
 - [12] W. Thirring, Ann. Phys. **3**, 91 (1958).
 - [13] S.Y. Lee, T. K. Kuo, and A. Gavrielides, Phys. Rev. D **12**, 2249 (1975).
 - [14] N. Boussaïd and S. Cuccagna, Comm. PDE **37**, 1001 (2012).
 - [15] D.E. Pelinovsky and Y. Shimabukuro, Lett. Math. Phys. **104**, 21 (2014).
 - [16] A. Contreras, D.E. Pelinovsky and Y. Shimabukuro, arXiv:1312.1019
 - [17] D.E. Pelinovsky and A. Stefanov, J. Math. Phys. **53**, 073705 (2012).
 - [18] A. Comech, T. Phan, and A. Stefanov, arXiv:1407.0606.
 - [19] N. Boussaïd and A. Comech, arXiv:1211.3336.
 - [20] J. Xu, S. Shao and H. Tang, J. Comp. Phys **245**, 131 (2013).
 - [21] S. Shao, N.R. Quintero, F.G. Mertens, F. Cooper, A. Khare, and A. Saxena, Phys. Rev. E **90**, 032915 (2014).
 - [22] F. Cooper, A. Khare, B. Mihaila, and A. Saxena, Phys. Rev. E **82**, 036604 (2010).

- [23] G. Berkolaiko and A. Comech, *Math. Model. Nat. Phenom.* **7**, 13 (2012).
- [24] J. Cuevas-Maraver, P.G. Kevrekidis, and A. Saxena, *J. Phys. A* **48**, 055204 (2015).
- [25] L. Haddad, K. O'Hara, and L.D. Carr, *Phys. Rev. A* **91**, 043609 (2015).
- [26] L. Haddad and L.D. Carr, *New J. Phys.* **17**, 113011 (2015).
- [27] T. O. Wehling, A. M. Black-Schaffer, and A. V. Balatsky, *Adv. Phys.* **63**, 1 (2014).
- [28] K. F. Mak, C. Lee, J. Hone, J. Shan, and T. F. Heinz, *Phys. Rev. Lett.* **105**, 136805 (2010).
- [29] M. J. Ablowitz, S.D. Nixon, and Y. Zhu, *Phys. Rev. A* **79**, 053830 (2009).
- [30] M. J. Ablowitz and Y. Zhu, *Phys. Rev. A* **82**, 013840 (2010).
- [31] O. Peleg, G. Bartal, B. Freedman, O. Manela, M. Segev, and D.N. Christodoulides, *Phys. Rev. Lett.* **98**, 103901 (2007).
- [32] M. Soler, *Phys. Rev. D* **1**, 2766 (1970).
- [33] D.J. Gross, and A. Neveu, *Phys. Rev. D* **10**, 3235 (1974).
- [34] G. Herring, L.D. Carr, R. Carretero-González, P.G. Kevrekidis, and D.J. Frantzeskakis, *Phys. Rev. A* **77**, 023625 (2008).
- [35] An expanded discussion of the associated existence and stability problems is given in the Supplementary Material.
- [36] L.N. Trefethen, *Spectral methods in MATLAB*. SIAM, Philadelphia (2000).
- [37] J. Cuevas-Maraver, P.G. Kevrekidis, A. Saxena, F. Cooper, A. Khare, A. Comech, and C.M. Bender, *J. Sel. Top. Quant. Electr.* **22**, 1 (2016); arXiv:1508.00852.
- [38] L. Lu, Z. Wang, D. Ye, L. Ran, L. Fu, J.D. Joannopoulos, M. Soljačić, *Science* **349**, 622 (2015).
- [39] D. Agueev and D. Pelinovsky, *SIAM J. Appl. Math.* **65**, 1101 (2005).